An online surface topography simulation model for single-point diamond turning considering relative tool-workpiece vibration and swelling effect

Gen-Shen Liu, Yuan-Liu Chen*, and Bing-Feng Ju

The State Key Lab of Fluid Power and Mechatronic Systems, Zhejiang University, 310027 Hangzhou, China
Corresponding E-mail: yuanliuchen@zju.edu.cn

KEYWORDS: Surface Topography, Single-point Diamond Turning, Vibration, Deep Learning, Online Monitoring

This paper presents an online simulation model for surface topography generation in single-point diamond turning process. During turning process, the relative tool-workpiece vibration was monitored by acquiring the internal signals of the machine tool from the motion controller, then a volumetric surface roughness model considering tool geometry, cutting parameters and relative vibration was developed. In addition, a deep learning model was adopted to account for the effects of plastic side flow and material spring back on the surface profile. By combining the two models above, an integrated online surface topography simulation model was constructed and its feasibility and prediction accuracy was verified by turning experiments. The modelling method presented in this work provided an important means for online surface quality monitoring in single-point diamond turning process.

1. Introduction

Single-point diamond turning (SPDT), introduced in the 1950s, is a crucial technology for making complex components in optics, photonics, and telecommunications[1]. It can produce surfaces with nanometric roughness and sub-micrometric accuracy, eliminating the need for post-polishing[1,2]. However, achieving such precision relies on factors like machine tool performance, working environment, cutting parameters, tool geometry, and material properties[3]. Therefore, a comprehensive surface roughness prediction model for SPDT should consider these factors to achieve accurate results.

In recent decades, significant work has gone into developing surface roughness prediction models for single-point diamond turning (SPDT). Early models focused on ideal cases which only considered the influence of tool nose radius and feedrate. However, these models did not account for tool-workpiece vibration, which Cheung addressed with a 3D simulation model considering steady harmonic motion[4]. Huang expanded this by incorporating vibration in both infeed and feeding directions, applicable to spherical and free-form surfaces, using vibration data from a built-in software of the machine tool[5,6]. Other researchers, like Cao, used acceleration sensors and grating rulers for collecting vibration data, while Chen extracted tool locus from surface profiles to determine equivalent amplitude of tool-work vibration[7,8].

Material swelling effect, including plastic side flow and elastic recovery, also significantly affects surface topography and roughness in SPDT. Experiments by To and Cheung showed that swelling effect distorts tool marks and correlates with surface roughness[9]. Kong's research indicated that elastic recovery is dominant for ductile materials, leading to lower roughness than theoretical predictions[10]. Liu developed a model for micro-turning that factors in plastic side flow, tool geometry, and process parameters, suggesting that discrepancies between theoretical and measured roughness are due to side flow[11].

2. Signal acquisition system and surface topography simulation model

2.1 Workflow of the proposed model

The workflow diagram in Fig. 1 outlines the signal acquisition and prediction process for the proposed model. The motion controller directs the motion of the machine tool according to the NC program while also receiving feedback signals from grating ruler sensors. Three internal signals (XRPOS signal, CRPOS signal, ZPE signal), collected at a fixed frequency f_s and duration ΔT, are selected for the use of surface topography simulation and stored in arrays by an ACSPL+

program within the controller. After each collection cycle, the controller communicates with the host computer via Ethernet, sending the data for further analysis using Python and MATLAB. This includes a surface topography simulation model considering relative vibration and a deep learning model accounting for material swelling effect. The host computer updates the prediction results dynamically as new data arrives every ΔT time interval.

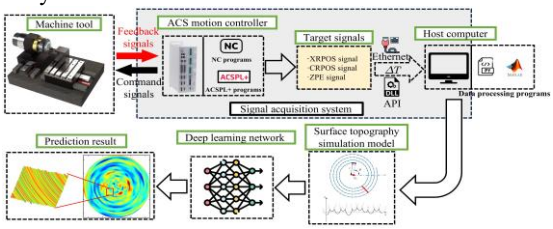

Fig. 1 Workflow of the proposed roughness prediction model

2.1 Surface topography simulation model

The surface topography simulation model in this study adopts a structure similar to previous ones, which divides the simulated surface into multiple radial sections[4,7]. Each section comprises a number of cutting points and these points are plotted in polar coordinates, with each point defined by its polar radius r, polar angle θ, and height z, based on XRPOS, CRPOS, and ZPE values respectively, as illustrated in Fig. 2. Unlike static models, this dynamic model updates simulation results during the cutting process using signal data from the motion controller. The simulation result starts as a ring-shaped area and finally becomes a disk area as the turning process completes. This allows for real-time monitoring and potential interruption if anomalies are detected, preventing damage to the workpiece or tool.

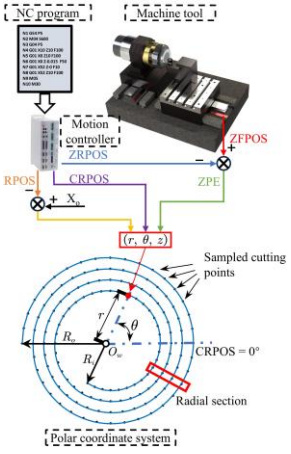

Fig. 2 Sampled cutting points plotted in the polar coordinate system

The different depths of the tool marks resulted from the relative vibration between the tool and the workpiece will lead to variational residual heights and thus a greater surface roughness. Vibration sources include tool tip, spindle, material-induced, tool holder, slide, and table vibrations. For the machine tool studied in this work, the relative tool-work vibration mainly comes from the slide vibration. Therefore, only Z-slide vibration (ZPE signal) is considered, as it represents the major part of the total relative tool-work vibration in face turning.

Fig. 4 illustrates the process of obtaining the radial sectional roughness profile using relative vibration data at each cutting point (the positions of the cutting points $T_i(X_i,\ Z_i)$). The feed distance L, represented by the length of each profile, is calculated using the outer radius R_o and inner radius R_i of the simulated area as

$$L = R_o - R_i \tag{1}$$

The profile is composed of discrete points $\mathbf{P} = \{p_1(x_1,\ z_1),\ p_2(x_2,\ z_2),\ \ldots,\ p_N(x_N,\ z_N)\}^T \in \mathbb{R}^{N\times 2}$ with spacing Δl in the feed direction. The tool nose contour is used to determine the height of these points which is expressed as

$$z(x) = \frac{x^2}{2r_n} \tag{2}$$

where r_n is the nose radius of the diamond tool. Considering potential interference from nonadjacent tool contours, especially with small feeds and large tool radii, the model accounts for six nearby tool contours to calculate the height of these discrete points. This approach allows for the prediction of roughness profiles for each radial section, ultimately simulating the entire ring-shaped area's surface topography.

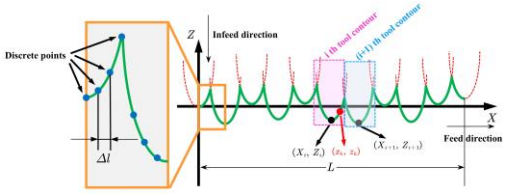

Fig. 3 The process of obtaining the radial sectional profile

3. Material swelling effect and LSTM prediction model

3.1 Surface topography simulation model

Fig. 4 shows the diamond turning process, where the existence of tool edge radius r_e causes a minimum cutting thickness $h_{\min}$. Below this thickness, materials don't form chips but experience burnishing and friction, leading to high pressure that forces some material to flow sideways while others indent to form the machined surface. Elastic recovery in the surface reduces roughness, while plastic side flow increases it. The swelling effect, a combination of these factors, is crucial for surface topography and must be considered in surface roughness prediction models for diamond turning, as it significantly impacts the finished surface, as reported in Zong's work[12].

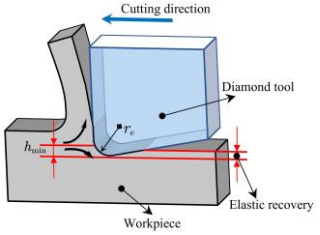

Fig. 4 Illustration of the cutting zone in diamond turning process in an orthogonal plane

Existing theoretical models for predicting elastic recovery or plastic side flow in surface roughness prediction require careful calibration of many coefficients, which significantly affect the model's accuracy. To address this, a deep LSTM network is proposed to predict the material swelling effect on the surface roughness profile, which is easier to train than calibrating empirical models. The network's output

can be directly used by the volumetric simulation model, simplifying the integration of the hybrid model.

3.2 Architecture of the designed deep LSTM network

To design a deep LSTM network for predicting surface roughness profiles influenced by material swelling, the network's input and output must be defined. The network aims to generate roughness profiles that match measured data by considering the swelling effect, using ideal radial section profiles from a volumetric simulation model as a basis. The input includes the ideal radial section profile and cutting parameters (depth of cut a_p, feedrate f_r, and cutting speed v_t), while the output is the modified profile. The network treats each discrete point of the radial section as a time step, with the input at each step being a vector of the cutting parameters and the output being the predicted profile height at that point. This approach allows the network to predict a modified radial section profile that accounts for the material swelling effect, as depicted in Fig. 5.

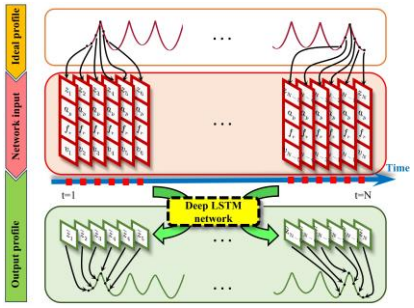

Fig. 5 Diagram of the input and output format of the deep LSTM network

The network architecture in Fig. 6 includes four Bi-directional LSTM (BiLSTM) layers, two fully connected (FC) layers, and input/output layers. BiLSTM layers process data in both directions, capturing past and future context, and are preferred over standard LSTM layers for this task. Each BiLSTM layer has 150 hidden and cell states. The last BiLSTM output uses a Leaky ReLU activation before entering the first FC layer with 300 neurons, followed by a second FC layer with 30 neurons, both using Leaky ReLU as activation function. Dropout layers with a 0.2 rate are added between BiLSTM layers to reduce overfitting. In Fig. 6, $\mathbf{h}_{\mathbf{b}}^{(\mathbf{a})}$ denotes the hidden state of the forward LSTM cell in a-th layer at b-th time step; $\mathbf{h}'^{(\mathbf{a})}_{\mathbf{b}}$ denotes the hidden state of the backward LSTM cell of a-th BiLSTM layer at b-th time step; $\mathbf{C}_{\mathbf{b}}^{(\mathbf{a})}$ represents the cell state of the forward cell of a-th BiLSTM layer at b-th time step and $\mathbf{C}'^{(\mathbf{a})}_{\mathbf{b}}$ is the cell state of the backward cell of a-th BiLSTM layer at b-th time step.

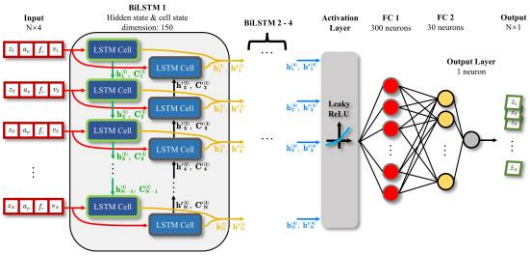

Fig. 6 Schematic of the architecture of the designed deep LSTM network

4. Experiment and result

4.1 Experimental setup

Face turning tests were conducted on a compact ultra-precision turning machine with T-shaped configuration and air-floating feed axes. A diamond tool with a 0° rake angle, 10° clearance angle, and 200μm nose radius was utilized. Red copper, chosen for its cleaner surface and fewer impurities, was used as the workpiece material, glued to an aluminum alloy part. The experimental setup is shown in Fig. 15.

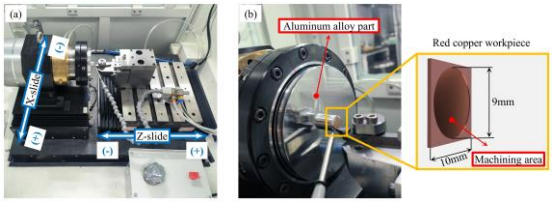

Fig. 7 Photographs of the experimental setup. (a) overall view; (b) close-up view

A frequency of 2kHz is used for internal signals collection, with data sampled for 5 seconds each cycle. Two groups of cutting experiments were conducted: Group A for training the deep LSTM network and Group B for testing the surface roughness prediction model. The cutting parameters for Group A are detailed in Table 1, with cutting speeds calculated for each position and input into the LSTM network. After each Group A experiment, surfaces were measured with a white-light interferometer, and roughness profiles were extracted. To train the LSTM network, both measured and ideal profiles are needed. An assumption was made that swelling effect deformations at all bottom points are consistent within the same radial profile, allowing for the reconstruction of ideal profiles, as shown in Fig. 8.

Table 1 Cutting parameters for experiments in Group A

Exp No.	Spindle speed (rpm)	Feed rate (μm/r)	Depth of cut (μm)
1	1000	4	2
2	1000	4	4
3	1000	4	6
4	1000	6	2
5	1000	6	4
6	1000	6	6
7	1000	8	2
8	1000	8	4
9	1000	8	6
10	1000	10	2
11	1000	10	4
12	1000	10	6
13	1000	12	2
14	1000	12	4
15	1000	12	6

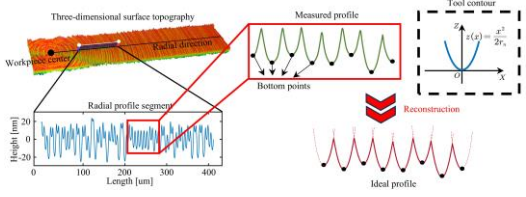

Fig. 8 Extracting profiles from measurement result and reconstruction of the ideal profile from measured profile

The cutting parameters of Group B, detailed in Table 2, differ from Group 1 to test the prediction model's generalization. After each experiment, surface topographies are measured and compared with predicted ones to validate the model's accuracy.

Table 2 Cutting parameters for experiments in Group B

Exp No.	Spindle speed (rpm)	Feed rate (μm/r)	Depth of cut (μm)
1	1000	5	2
2	1000	7	3
3	1000	11	3
4	1000	9	4
5	1000	5	5
6	1000	9	6

4.2 Prediction result

Fig. 9 shows 20 selected 0.42mm×0.42mm areas on the machined surface used to compare measurement and prediction results. Fig. 10 illustrates the model's predictions during experiment 5 in Group B, showing the evolution of the surface roughness (Sa) distribution diagram with the proceeding of the cutting process. The model enables real-time surface generation simulation and roughness monitoring, with rougher areas highlighted in red, indicating potential anomalies. Three areas were compared, demonstrating the model's ability to reflect actual surface topography.

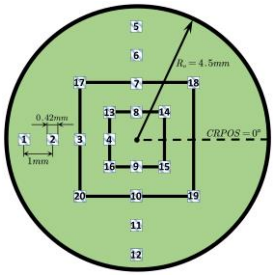

Fig. 9 Illustration of the selected local areas

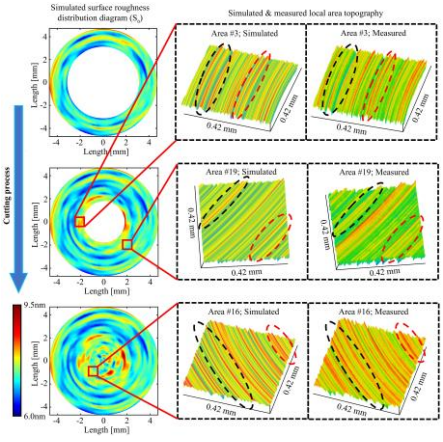

Fig. 10 Prediction result of the model with the proceeding of cutting process

5. Conclusions

This paper introduces a new surface roughness prediction model for single-point diamond turning that considers relative vibration and material swelling effects. A dynamic volumetric model simulates surface generation in real-time, and a deep LSTM network models the swelling effect on surface roughness. Two experiment groups—one for training and one for validation—show the model's accuracy. The model also provides in-process monitoring of surface roughness, demonstrating deep learning's potential in analyzing the swelling effect's impact on surface topography.

ACKNOWLEDGEMENT

This work was supported by the National Natural Science Foundation of China project "Fundamental Research on Fast Tool Servo Technology for Cross-Scale Ultra-Precision Machining with Full-Drive Chain Sensing Feedback".

REFERENCES

1. N. Ikawa, R.R. Donaldson, R. Komanduri, W. König, T.H. Aachen, P. A. McKeown, T. Moriwaki, I.F. Stowers, “Ultra-precision metal cutting–the past, the present and the future,” CIRP Ann.– Manuf. Technol., Vol. 40, pp. 587–594, 1991.
2. C.F. Cheung, W.B. Lee, “Study of factors affecting the surface quality in ultraprecision diamond turning,” Mater. Manuf. Process., Vol. 15, No. 4, pp. 481-502, 2000.
3. D. Dornfeld, S. Min, Y. Takeuchi, “Recent advances in mechanical micromachining,” CIRP Ann.– Manuf. Technol., Vol. 55, No. 2, pp. 745–768, 2006.
4. C. F. Cheung, W.B. Lee, “Modelling and simulation of surface topography in ultra-precision diamond turning,” Proc. Inst. Mech. Eng. Pt. B: J. Eng. Manuf., Vol. 214, No. 6, pp. 463–80, 2000.
5. Chih-Yu Huang, Rongguang Liang, “Modeling of surface topography in single-point diamond turning machine,” Appl. Opt., Vol. 54, No. 23, pp. 6979-85, 2015.
6. Chih-Yu Huang, Rongguang Liang, “Modeling of surface topography on diamond-turned spherical and freeform surfaces,” Appl. Opt., Vol. 56, No. 15, pp. 4466-4473, 2017.
7. Yang Cao, Xuesen Zhao, Guo Li, Wenjun Zong, Tao Sun, “Study regarding the influence of process conditions on the surface topography during ultra-precision turning,” J. Manuf. Process., Vol. No. 102, pp. 23-36, 2023.
8. Junyun Chen, Qingliang Zhao, “A model for predicting surface roughness in single-point diamond turning,” Measurement., Vol. 69, pp. 20-30, 2015.
9. S. To, C. F. Cheung, W. B. Lee, “Influence of material swelling on surface roughness in diamond turning of single crystals,” Mater. Sci. Technol., Vol. 17, pp. 102-108, 2001.
10. M. C. Kong, W. B. Lee, C. F. Cheung, S. To, “A study of materials swelling and recovery in single-point diamond turning of ductile materials,” J. Mater. Process. Tech., Vol. 180, pp. 210-215, 2006.
11. Kai Liu, Shreyes N. Melkote, “Effect of plastic side flow on surface roughness in micro-turning process,” Int. J. Mach. Tools Manuf., Vol. 46, pp. 1778–1785, 2006.
12. W. J. Zong, Y. H. Huang, Y. L. Zhang, T. Sun, “Conservation law of surface roughness in single point diamond turning,” Int. J. Mach. Tools Manuf., Vol. 84, pp. 58-63, 2014.